

# Contrast measure improved by weighted vertical mean difference for small infrared maritime target detection

Xun Zhang<sup>a,b</sup>, Xingtai Yue<sup>b</sup>, Zheng Li<sup>b</sup>, Yan Zheng<sup>\*a</sup>

<sup>a</sup>College of Intelligent Systems Science and Engineering, Harbin Engineering University, Harbin 150001, Heilongjiang, China; <sup>b</sup>Qingdao Innovation and Development Center, Harbin Engineering University, Qingdao 266000, Shandong, China

## ABSTRACT

A weighted vertical difference contrast measure (WVDCM) for small infrared maritime target detection is proposed for the complex background of the sea surface and the difficulty of infrared weak target detection under environmental interference conditions. The algorithm firstly adopts a multi-scale vertical mean difference filtering method with weighted information entropy to pre-process the images. Secondly, the multi-scale patch local contrast method with human visual system (HVS) is utilized for enhancing the detection target while suppressing the background, and ultimately, the adaptive threshold segmentation method is employed to acquire the actual target. The results of the simulation experiments of this algorithm on the sea surface data-set show that the image's get higher detection rate under the condition of low false alarm rate, and the signal-to-clutter ratio gain (SCRg) and background suppression factor (BSF) of the image are more obviously improved than other algorithms.

**Keywords:** Spatial filtering, information entropy, infrared target detection, human visual system (HVS), weighted vertical difference contrast measure (WVDCM)

## 1. INTRODUCTION

With the advancement of infrared imaging technology (IRST) and the growing military demand for sea surface target tracking and monitoring, there is an increasingly urgent demand for small infrared maritime target detection technology<sup>1</sup>. Therefore, IR small target detection algorithms that satisfy low false alarm rate and high detection accuracy in complex backgrounds on the sea surface are increasingly receiving wide attention from researchers at home and abroad<sup>2</sup>. Compared with other targets, small IR maritime target have two characteristics<sup>3</sup>, on the one hand, due to the complex background of the sea surface and the influence of the electronic characteristics of IR cameras, resulting in low signal-to-clutter ratio and small difference between the target and the background, showing “weak” characteristics<sup>4</sup>. On the other hand, due to the military need to detect target at long distances, the imaging distance is long<sup>5</sup>, and the target occupies only a few pixels of the image, presenting a “small” characteristic. It is also due to these two characteristics that make the detection of small IR maritime target more difficult<sup>6</sup>.

The small IR target detection algorithms are mainly classified into multi-frame detection, single-frame detection<sup>7</sup> and intelligent detection based on deep learning<sup>8</sup>. However, the small size of the target, the lack of feature information, and the difficulty of collecting data sets on the sea surface make the neural network limited in the work of small IR maritime target detection<sup>9</sup>, so the intelligent detection algorithm based on deep learning cannot be fully applied to the detection of small IR targets on the sea surface. There are several multi-frame detection methods such as temporal profiles<sup>10</sup>, maximum-likelihood estimation<sup>11</sup>, generalized likelihood ratio test<sup>12</sup>, dynamic program algorithm<sup>13</sup>, Markov random field<sup>14</sup>. And compared with multi-frame detection, single-frame detection has the features of high detection efficiency and easy implementation. In recent years researchers both domestically and internationally have focused on single-frame detection research<sup>15</sup>.

In recent years, the human visual system (HVS) has received wide attention, and research scholars found that its contrast mechanism is very suitable for the field of infrared weak target detection, Chen et al.<sup>16</sup> proposed the local contrast method (LCM), which first applied the contrast mechanism to infrared weak target detection, and then Han et al. improved the LCM method and proposed Improved local contrast measure (ILCM)<sup>17</sup>, relative local contrast

\*yanzheng3@hrbeu.edu.cn; phone 13573836456

measure(RLCM)<sup>18</sup>, and novel local contrast measure(NLCM)<sup>19</sup>, respectively. Wei et al.<sup>20</sup> proposed a multi-scale patch contrast method based on LCM (MPCM), which can detect both bright targets and dark targets, and achieved better detection results. However, the detection performance of the above algorithm degrades in the case of strong background interference. In addition, Xia et al.<sup>21</sup> combined local contrast with the random wandering method, Han et al.<sup>22</sup> combined local contrast with adaptive background estimation, and also proposed the local contrast metric (TLLCM) under a three-layer window (TLLCM)<sup>23</sup>. However, none of the above methods can achieve the best detection results for the detection of weak IR targets on the sea surface. Yang<sup>24</sup> propose a novel IR maritime target detection method called weighted multi-directional gradient (WMDG) measure, this method is more suitable for surface IR weak target detection.

Considering the above analysis, we proposed an improved IR maritime target detection method called weighted vertical difference contrast measure (WVDCM). This paper is influenced by Reference<sup>16</sup> algorithm, we firstly propose a multi-scale vertical mean difference filtering method and weight the filtered images after filtering using local information entropy. Additionally, a multi-scale block local contrast approach is employed to enhance the target while mitigating background interference. Subsequently, an adaptive threshold segmentation technique is utilized to isolate the actual target. This approach significantly reduces the impact of high-brightness pixel-sized noise (PNHB) and ensures a low false alarm rate in intricate maritime backgrounds. Moreover, it facilitates the detection of maritime targets of varying sizes, addressing challenges related to size diversity and enhancing both the robustness and versatility of the algorithm. The experimental results demonstrate that, in comparison with alternative approaches, the proposed method exhibits superior efficiency in extracting genuine targets on the sea surface.

## 2. PROPOSED ALGORITHM

The flowchart in Figure 1 gives the structure of the proposed algorithm in this paper. Let the input image be  $F$ . First, the input image is filtered using the multi-scale vertical mean difference, and the filtered image is denoted as  $S$ . Meanwhile, the local information entropy of the input image is calculated to obtain  $E$ . The output result of this step is denoted as  $I$ . Then  $I$  is the product of the square of the filtered pixel value and the local information entropy, i.e.,  $I=S^2 \times E$ . Subsequently, the multi-scale local contrast is calculated for  $I$  to obtain the salient map  $C$ . Finally, an adaptive threshold segmentation of  $C$  is performed to extract the real target.

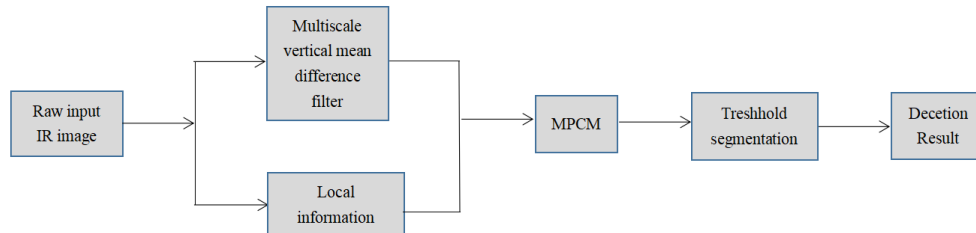


Figure 1. The flowchart of our method.

### 2.1 Multi-scale vertical mean difference filtering

When the infrared weak target detection algorithm is applied to military applications on the sea surface, the target is usually enemy ships. The characteristics of this type of target in the infrared image are that the only bright spot is prominent and radiates to the surrounding areas, which presents a Gaussian distribution feature.

This article proposes a vertical mean difference filter that fully utilizes the Gaussian distribution of infrared small and weak targets. In the pre-processing stage, the original image is filtered to pre-liminarily filter out obvious background clutter to improve the accuracy of feature extraction, thereby reducing false alarm rates and improving detection accuracy.

The International Society for Optics Engineering (SPIE) refers to targets with no more than 80 pixels as small targets<sup>14</sup>, which have a maximum size of  $9 \times 9$  (pixels). As mentioned earlier, the change in target size is one of the important reasons why many algorithms cannot accurately detect real targets. Therefore, this article designs  $3 \times 3$ ,  $5 \times 5$ ,  $7 \times 7$ ,  $9 \times 9$ . Four multi-scale vertical mean difference filters are used for multi-scale filtering.

Assuming the input image is  $F$ , the center point is  $(x, y)$ , and  $m_i$  and  $d_i$  ( $i=1, 2, 3, 4$ ) represent the vertical mean and vertical mean difference of the four scales, respectively:

$$m_i = \frac{1}{4}[F(x-i, y) + F(x+i, y) + F(x, y-i) + F(x, y+i)] \quad (1)$$

$$d_i = F(x, y) - m_i \quad (2)$$

$$F(x, y) = d = (\max\{d_i\})^2 \quad (3)$$

The vertical mean difference filter designed based on the above formula is shown in the Figure 2 (with 3×3 scales as an example). Due to the influence of thermal radiation, infrared small targets usually appear as bright spots in grayscale images. Squaring operation can avoid the situation where the central area is dark and the d value is negative.

	$-\frac{1}{4}$	
$-\frac{1}{4}$	1	$-\frac{1}{4}$
	$-\frac{1}{4}$	

Figure 2. With 3×3 scales as an example.

## 2.2 Local information entropy

The information contained in the information source can be determined by utilizing local information entropy, which serves as a measure of the amount of information within a specific range<sup>15</sup>. For a window, its local information entropy is defined as:

$$E = -\sum_{i=0}^{M-1} p_i \log_2 p_i \quad (4)$$

where  $p_i$  is the probability density function of the  $i$ th gray level in the window, and  $M$  is the maximum gray level of the window. For flat and similar background areas, this value is small, while for heterogeneous target areas, this value is large. Considering the characteristics of infrared dim small targets, this paper sets the local information entropy window as 9×9. Weighting the above processed image by local information entropy (as shown in the following formula), the initial salient image is obtained.

$$I(x, y) = F(x, y) \times E(x, y) \quad (5)$$

## 2.3 Muti-scale patch local contrast

The concept of local contrast has been widely applied in the field of pattern recognition. In 2014, Chen et al. proposed a Local Contrast Method<sup>16</sup> (LCM), The application of which in infrared weak target detection is introduced for the first time, yielding favorable detection results. This approach employs a sliding window to systematically traverse the entire infrared image pixel by pixel, proceeding from top to bottom and left to right. (as shown in Figure 2), and calculates the local contrast of each pixel point. Finally, the calculated local contrast operator is used as the feature of the pixel point for threshold segmentation to obtain the true target to be detected.

From Figure 3, it can be seen that the sliding window is divided into nine 3×3 sub windows, where the center sub window T represents the area where the target may appear,  $B_i$  ( $i=1, 2... 8$ ) represents the background area, and  $m_i$  ( $i=1, 2... 8$ ) represents the average gray level of each background area, that is:

B1	B2	B3
B8	T	B4
B7	B6	B5

Figure 3. The window proposed in LCM.

$$m_i = \frac{1}{N} \sum_{j=1}^N I_j^i \quad (6)$$

where  $N$  is the number of pixels in sub window  $j$ ,  $I_j^i$  representing the grayscale value of the  $j$ th pixel in the  $i$ th background area. The contrast between the central window and its adjacent 8 background areas is defined as:

$$c_i = \frac{L_0}{m_i} \quad (7)$$

where  $L_0$  is the maximum grayscale value of the target window. In summary, the expression for the LCM operator is:

$$C = \min_i (L_0 \times c_i) = \min_i (L_0 \times \frac{L_0}{m_i}) = \min_i (\frac{L_0^2}{m_i}) \quad (8)$$

The above formula indicates that the larger  $C$ , the more likely the pixel is to have a target. However, due to the use of only the maximum grayscale value of the central window and the square operation, when there are large pulses or interference from bright noise, the detection false alarm rate is high and the detection effect is poor.

In response to the problems in LCM, Wei<sup>9</sup> proposed a multi-scale patch contrast method, which provides a nested structure (as shown in Figure 3) and defines the difference between the target region  $T$  and the background region  $B_i$  as:

$$D(T) = \begin{pmatrix} d(T, B1) \\ d(T, B2) \\ \vdots \\ d(T, B8) \end{pmatrix} \quad (9)$$

$$d(T, B_i) = m_T - m_{B_i}, (i = 1, 2, \dots, 8) \quad (10)$$

Among them,  $m_T$  and  $m_{B_i}$  represent the grayscale mean of the central patch and the  $i$ th domain background, respectively.

The difference between the center area and the background area in the  $i$ -th direction is defined as  $d_i$ , and the  $d_i$  calculation formula is:

$$d_i = d(T, B_i) \times d(T, B_i + 4), (i = 1, 2, \dots, 4) \quad (11)$$

$$C(x, y) = \min_{i=1,2,\dots,4} d_i \quad (12)$$

After the image  $I$  filtered by the multi-scale vertical mean difference weighted by information entropy, the above MPCM processing is performed again to obtain the significance graph  $C$ .

## 2.4 Adaptive threshold segmentation

The region in the final feature map with the highest feature value is highly likely to be the target region, and an adaptive threshold segmentation method is employed for extracting the actual target to be detected.

$$u_C = \frac{1}{m \times n} \sum_{i=1}^m \sum_{j=1}^n C(i, j) \quad (13)$$

$$\sigma_C = \frac{1}{m \times n} \sum_{i=1}^m \sum_{j=1}^n [C(i, j) - u_C]^2 \quad (14)$$

$$T_h = u_C + k \times \sigma_C \quad (15)$$

In the equation,  $m$  and  $n$  denote the number of rows and columns in the image, respectively.  $C(i, j)$  is the salient image obtained through the above calculation, where,  $u_C$  and  $\sigma_C$  represent the mean and variance of the salient image,  $k$  is an adaptive parameter, and  $T_h$  is the calculated threshold. After threshold segmentation, the real target to be detected is extracted.

### 3. EXPERIMENTAL RESULT

#### 3.1 Evaluation criteria

To assess the efficacy of the algorithm, background suppressor (BSF) and signal-to-clutter ratio gain (SCRg) are employed as evaluation metrics.

$$SCR = \frac{\mu_t - \mu_b}{\sigma_b} \quad (16)$$

$$SCRg = \frac{SCR_{out}}{SCR_{in}} \quad (17)$$

$$BSF = \frac{\sigma_{in}}{\sigma_{out}} \quad (18)$$

The average pixel value of the target region and the background region is represented by  $\mu_T$  and  $\mu_B$  respectively, while  $\sigma_B$  represents the standard deviation of the background region. The subscripts in and out denote the input image and output image respectively. According to the above formula, it can be seen that SCRg can represent the ability of algorithm to enhance real targets, while BSF can represent the algorithm's ability to suppress background. Usually, the larger the values of SCRg and BSF, the more prominent the target is in the image.

In addition, ROC curves were used to depict the relationship between the detection rate  $P_d$  and the false detection rate  $P_f$ , where

$$p_d = \frac{\text{number of detected actual targets}}{\text{number of total actual targets}} \quad (19)$$

$$p_f = \frac{\text{number of false alarm targets}}{\text{number of total detected targets}} \quad (20)$$

In the ROC curve, a higher number of detection curves in the upper left corner indicates better detection effectiveness, and a larger area under the curve signifies superior algorithm performance. Hence, the area under the curve (AUC) is also employed as a crucial indicator reflecting algorithm performance.

#### 3.2 Experimental findings

In this paper, four of the most progressive infrared small target detection algorithms are selected as comparison methods, including, MPCM<sup>20</sup>, RLCM<sup>18</sup>, TLLCM<sup>23</sup>, tophat<sup>25</sup>, WMDG<sup>24</sup>. Firstly, for the three different complex sea surface environments shown in Figure 4, Figure 5 presents the salient maps and corresponding 3D maps obtained by six methods, including the algorithm proposed in this paper. Secondly, Tables 1 and 2 respectively provide the SRCg and BSF of four baseline algorithms and the algorithms proposed in this paper. According to Tables 1 and 2, The algorithm proposed in this paper achieves the maximum SCRg and BSF for three different complex sea surface background situations, as evidenced by our findings. As shown in Figure 6, the algorithm proposed in this paper also has the highest AUC among the comparison algorithms. That is to say, the algorithm proposed in this paper outperforms the other four baseline algorithms in both target enhancement and background suppression.



Figure 4. Image1-2.

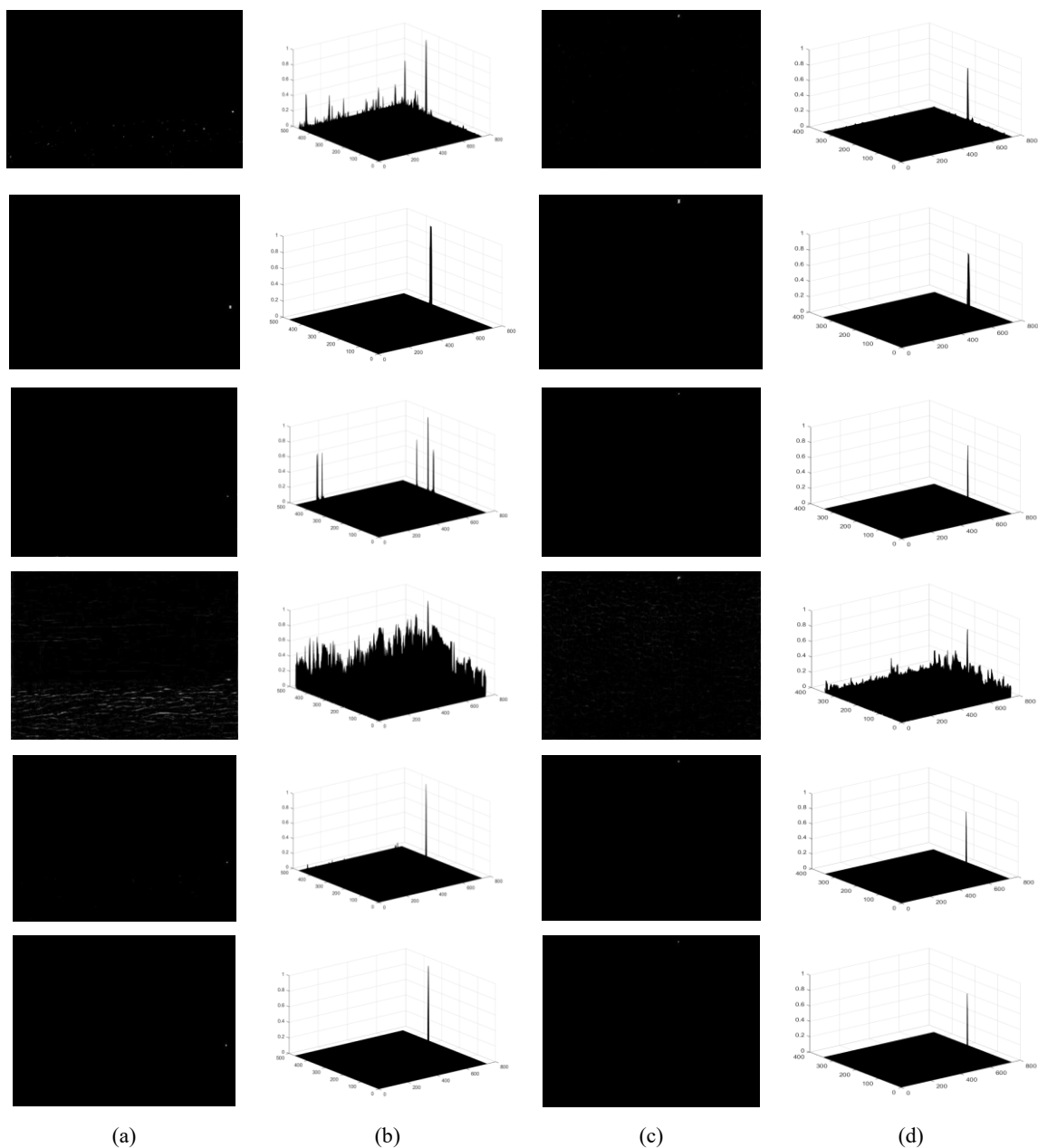


Figure 5. (a, b): The significance and 3D plots obtained by each method for image1; (c, d): The significance and 3D plots obtained by each method for image2.

Note: The top to bottom processing methods are MPCM, RLCM, TLLCM, TOPHAT, WMDG and proposed.

Table 1. SCRG of different algorithms.

	<b>MPCM</b>	<b>RLCM</b>	<b>TLLCM</b>	<b>TOPHAT</b>	<b>WMDG</b>	<b>Proposed</b>
Dataset1	25.2721	48.1484	91.5020	2.5630	125.8965	<b>237.0231</b>
Dataset2	20.0873	23.7892	32.5625	3.5475	<b>167.8600</b>	133.9136
Average	23.2682	38.7335	68.7217	2.9435	142.1155	<b>197.1710</b>

Table 2. BSF of different algorithms.

	<b>MPCM</b>	<b>RLCM</b>	<b>TLLCM</b>	<b>TOPHAT</b>	<b>WMDG</b>	<b>Proposed</b>
Dataset1	8.8047	6.8539	10.4397	1.1727	15.3874	<b>16.0542</b>
Dataset2	5.5183	3.7738	6.1511	1.1915	9.4923	<b>10.3939</b>
Average	7.5345	5.6634	8.7821	1.1800	13.1089	<b>13.8665</b>

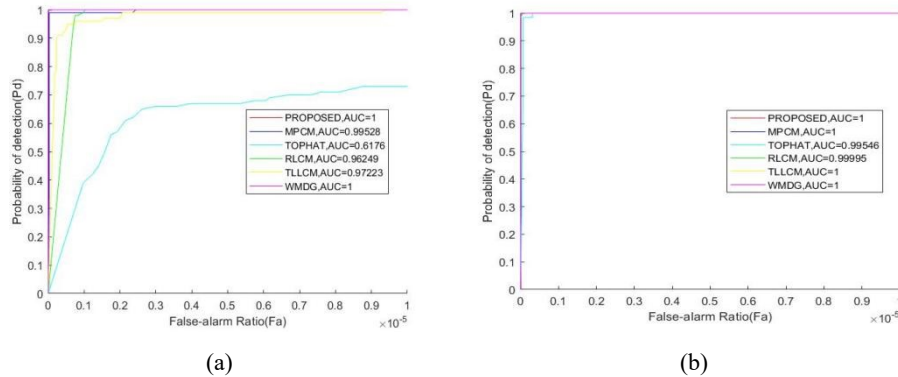


Figure 6. ROC curves of the six methods on two datasets.

#### 4. CONCLUSIONS

In this paper, we introduce a novel approach termed the multi-scale weighted vertical mean difference filter combined with a local contrast mechanism (WVDCM) for detecting weak small infrared targets. Prior to the local contrast calculation, we design a vertical mean difference filter tailored to the characteristics of small targets and employ information entropy weighting on the filtered images. Subsequently, most background clutter is effectively filtered out while enhancing the real target. The final step involves extracting the target using the local contrast mechanism in HVS. Experimental results demonstrate that our proposed algorithm exhibits strong detection capabilities in complex sea surface backgrounds.

#### ACKNOWLEDGMENT

This work is supported by NSFC Grant No. 62101156 and Natural Science Foundation of Shandong Province No. ZR2022ME104.

#### REFERENCES

- [1] Chen, Y. W., Song, B., Wang, D. J. and Guo, L. H., "An effective infrared small target detection method based on the human visual attention," *Infrared Physics & Technology* 95, 128-135 (2018).
- [2] Dong, L., Wang, B., Zhao, M. and Xu, W., "Robust infrared maritime target detection based on visual attention and spatiotemporal filtering," *IEEE Transactions on Geoscience and Remote Sensing* 55, 3037-3050 (2017).
- [3] Lu, Y., Dong, L., Zhang, T. and Xu, W., "A robust detection algorithm for infrared maritime small and dim targets," *Sensors* 20, 1237 (2020).
- [4] Yang, P., Dong, L. and Xu, W., "Infrared small maritime target detection based on integrated target saliency measure," *IEEE Journal of Selected Topics in Applied Earth Observations and Remote Sensing* 14, 2369-2386 (2021).
- [5] Yang, C., Ma, J., Qi, S., Tian, J., Zheng, S. and Tian, X., "Directional support value of Gaussian transformation for infrared small target detection," *Applied Optics* 54, 2255-2265 (2015).

- [6] Bi, Y., Bai, X., Jin, T. and Guo, S., "Multiple feature analysis for infrared small target detection," *IEEE Geoscience and Remote Sensing Letters* 14, 1333-1337 (2017).
- [7] Gao, C., Meng, D., Yang, Y., Wang, Y., Zhou, X. and Hauptmann, A. G., "Infrared patch-image model for small target detection in a single image," *IEEE Transactions on Image Processing* 22, 4996-5009 (2013).
- [8] Qian, K., Zhou, H., Qin, H., Rong, S., Zhao, D. and Du, J., "Guided filter and convolutional network-based tracking for infrared dim moving target," *Infrared Physics & Technology* 85, 431-442 (2017).
- [9] Wang, X. and Zhang, T., "Clutter-adaptive infrared small target detection in infrared maritime scenarios," *Optical Engineering* 50, (2011).
- [10] Liu, D., Li, Z., Wang, X. and Zhang, J., "Moving target detection by nonlinear adaptive filtering on temporal profiles in infrared image sequences," *Infrared Physics & Technology* 73, 41-48 (2015).
- [11] Balasingam, B., Bar-Shalom, Y., Willett, P. and Pattipati, K., "Maximum likelihood detection on images," In *Proceedings of the 20th International Conference on Information Fusion*, 10-13 July 2017, Xi'an, China, (2017).
- [12] Nichols, J. M., "An improved GLRT for image-based point source detection and estimation," *IEEE Transactions on Aerospace and Electronic Systems* 53, 1536-1544 (2017).
- [13] Sun, X., Liu, X., Tang, Z., Long, G. and Yu, Q., "Real-time visual enhancement for infrared small dim targets in video," *Infrared Physics & Technology* 83, 217-226 (2017).
- [14] Gao, C., Wang, L., Xiao, Y., Zhao, Q. and Meng, D., "Infrared small-dim target detection based on Markov random field guided noise modeling," *Pattern Recognition* 76, 463-475 (2018).
- [15] Wang, X., Peng, Z., Kong, D. and He, Y., "Infrared dim and small target detection based on stable multisubspace learning in heterogeneous scene," *IEEE Transactions on Geoscience and Remote Sensing* 55, 5481-5493 (2017).
- [16] Chen, C. L. P., Li, H., Wei, Y., Xia, T. and Tang, Y. Y., "A local contrast method for small infrared target detection," *IEEE Trans. Geoscience and Remote Sensing* 52, 574-581 (2014).
- [17] Han, J., Ma, Y., Zhou, B., Fan, F., Liang, K. and Fang, Y., "A robust infrared small target detection algorithm based on human visual system," *IEEE Geoscience and Remote Sensing Letters* 11, 2168-2172 (2014).
- [18] Han, J., Liang, K., Zhou, B., Zhu, X., Zhao, J. and Zhao, L., "Infrared small target detection utilizing the multiscale relative local contrast measure," *IEEE Geoscience and Remote Sensing Letters* 15, 612-616 (2018).
- [19] Qin, Y. and Li, B., "Effective infrared small target detection utilizing a novel local contrast method," *IEEE Geoscience and Remote Sensing Letters* 13, 1890-1894 (2016).
- [20] Wei, Y., You, X. and Li, H., "Multiscale patch-based contrast measure for small infrared target detection," *Pattern Recognition* 58, 216-226 (2016).
- [21] Xia, C., Li, X. and Zhao, L., "Infrared small target detection via modified random walks," *Remote Sensing* 10, 2004 (2018).
- [22] Han, J., Liu, S., Qin, G., Zhao, Q., Zhang, H. and Li, N., "A local contrast method combined with adaptive background estimation for infrared small target detection," *IEEE Geoscience and Remote Sensing Letters* 16, 1442-1446 (2019).
- [23] Han, J., Moradi, S., Faramarzi, I., Liu, C., Zhang, H. and Zhao, Q., "A local contrast method for infrared small-target detection utilizing a Tri-Layer window," *IEEE Geoscience and Remote Sensing Letters* 17, 1822-1826 (2020).
- [24] Yang, P., Dong, L. and Xu, W., "Detecting small infrared maritime targets overwhelmed in heavy waves by weighted multidirectional gradient measure," *IEEE Geoscience and Remote Sensing Letters* 19, 7002005 (2022).
- [25] Deshpande, S. D., Er, M. H., Ronda, V. and Chan, P., "Max-mean and max-median filters for detection of small-targets," In *Proceedings of the 1999 Signal and Data Processing of Small Targets*, 20-22 July 1999, 74-83 (1999).